A&A 557, A78 (2013)
DOI: 10.1051/0004-6361/201321920
© ESO 2013

Astronomy & Astrophysics

The ALHAMBRA survey: Discovery of a faint QSO at $z = 5.41$ *(Research Note)*

I. Matute[1], J. Masegosa[1], I. Márquez[1], A. Fernández-Soto[2,3], C. Husillos[1], A. del Olmo[1], J. Perea[1], M. Pović[1], B. Ascaso[1], E. J. Alfaro[1], M. Moles[1,4], J. A. L. Aguerri[5], T. Aparicio-Villegas[6], N. Benítez[1], T. Broadhurst[7], J. Cabrera-Cano[1,8], F. J. Castander[9], J. Cepa[5,10], M. Cerviño[1,5], D. Cristóbal-Hornillos[1,4], L. Infante[11], R. M. González Delgado[1], V. J. Martínez[3,12,13], A. Molino[1], F. Prada[1], and J. M. Quintana[1]

[1] Instituto de Astrofísica de Andalucía (CSIC), Glorieta de la Astronomía s/n, 18008 Granada, Spain
e-mail: [matute;isabel;pepa;cesar;chony;jaime;mpovic;emilio;benitez;mcs;rosa;amb;fprada;quintana]@iaa.es
[2] Instituto de Física de Cantabria (CSIC-UC), 39005 Santander, Spain
e-mail: fsoto@ifca.unican.es
[3] Unidad Asociada Observatori Astronòmic (IFCA – Universitat de València), Valencia, Spain
[4] Centro de Estudios de Física del Cosmos de Aragón (CEFCA), 44001 Teruel, Spain
e-mail: [moles;dch]@cefca.es
[5] Instituto de Astrofísica de Canarias, La Laguna, 38200 Tenerife, Spain
e-mail: jalfonso@iac.es
[6] Observatrio Nacional-MCT, CEP 20921-400, Rio de Janeiro-RJ, Brazil
e-mail: villegas@on.br
[7] School of Physics and Astronomy, Tel Aviv University, Israel
e-mail: tjb@wise.tau.ac.il
[8] Facultad de Física. Departamento de Física Atómica, Molecular y Nuclear, Universidad de Sevilla, 41012 Sevilla, Spain
e-mail: jcc-famn@us.es
[9] Institut de Ciències de l'Espai, IEEC-CSIC, 08193 Barcelona, Spain
e-mail: fjc@ieec.fcr.es
[10] Departamento de Astrofísica, Facultad de Física, Universidad de la Laguna, Spain
e-mail: jcn@iac.es
[11] Departamento de Astronomía, Pontificia Universidad Católica, 782-0436 Macul, Santiago, Chile
e-mail: linfante@astro.puc.cl
[12] Departament d'Astronomía i Astrofísica, Universitat de València, 46100 Valencia, Spain
e-mail: vicent.martinez@uv.es
[13] Observatori Astronòmic de la Universitat de València, 46071 Valencia, Spain

Received 19 May 2013 / Accepted 12 July 2013

ABSTRACT

Aims. We aim to illustrate the potentiality of the Advanced Large, Homogeneous Area, Medium-Band Redshift Astronomical (ALHAMBRA) survey to investigate the high-redshift universe through the detection of quasi stellar objects (QSOs) at redshifts higher than 5.

Methods. We searched for QSOs candidates at high redshift by fitting an extensive library of spectral energy distributions – including active and non-active galaxy templates, as well as stars – to the photometric database of the ALHAMBRA survey (composed of 20 optical medium-band plus the 3 broad-band JHK_s near-infrared filters).

Results. Our selection over ≈1 square degree of ALHAMBRA data (∼1/4 of the total area covered by the survey), combined with GTC/OSIRIS spectroscopy, has yielded identification of an optically faint QSO at very high redshift ($z = 5.41$). The QSO has an absolute magnitude of ∼−24 at the 1450 Å continuum, a bolometric luminosity of $\approx 2 \times 10^{46}$ erg s^{-1}, and an estimated black hole mass of $\approx 10^8$ $M_\odot$. This QSO adds itself to a reduced number of known UV faint sources at these redshifts. The preliminary derived space density is compatible with the most recent determinations of the high-z QSO luminosity functions. This new detection shows how ALHAMBRA, as well as forthcoming well-designed photometric surveys, can provide a wealth of information on the origin and early evolution of this kind of object.

Key words. galaxies: active – quasars: general – galaxies: distances and redshifts – galaxies: high-redshift – galaxies: evolution – quasars: emission lines

1. Introduction

It is now widely accepted that the release of gravitational energy, as matter falls into a supermassive black hole ($\sim 10^{6-9} M_\odot$; SMBH), is the main generation mechanism for the high luminosities observed in AGN. Inside the variety of the AGN family, quasi-stellar objects (quasars or QSOs) are the fraction that show particularly high intrinsic luminosities that allow them to be detected over very large distances. Consequently, QSOs provide a way to peer into the physical conditions of an early universe and study the history of the QSOs and their host galaxy interaction over cosmic time. The largest samples of known QSOs are

provided by the optical spectroscopic surveys carried out over thousands of sq. degrees of sky (e.g. SDSS and the 2dF QSO survey, 2QZ). These surveys secure tens of thousands of QSO detections and are able to derive detailed luminosity functions up to $z \sim 3$–4 (e.g., Richards et al. 2006b; Siana et al. 2008; Croom et al. 2009; Ross et al. 2013) in the form of double power laws with a characteristic luminosity (M^*) and faint and bright slopes (α and β for $M > M^*$ and $M < M^*$, respectively). The situation at very high-z ($z \gtrsim 5$) is quite different. At these redshifts, most of the identified QSOs (~300 objects above $z \sim 5$ and ~40 at $z > 6$) sample only the brightest end of the QSO luminosity function (QLF; Wolf et al. 2003; Fan et al. 2006; Jiang et al. 2009; Willott et al. 2010b; McGreer et al. 2013; Pâris et al. 2012). Over the redshift range $z = [5.0, 6.2]$, fewer than 10% of the known QSOs (23 objects; Mahabal et al. 2005; Jiang et al. 2009; Willott et al. 2010b; Masters et al. 2012; McGreer et al. 2013) sample the faint part of the QLF ($M_{1450} > -25$ where M_{1450} is the monocromatic luminosity at rest frame 1450 Å). This not only restrains our knowledge of the true number of faint QSOs at these redshifts but also severely hampers the derived accuracy of the overall QLF (given the high correlation between the LF parameters). This uncertainty in the high-z QLF limits our ability to answer some important cosmological questions, such as the contribution of QSOs to the epoch of re-ionization (Fan et al. 2006; Dunkley et al. 2009; Schroeder et al. 2013), the formation of SMBHs within the first billion years of the universe and its challenge to models of galaxy formation, BH formation, and BH growth (Di Matteo et al. 2005; Hopkins et al. 2010; Melia 2013; Khandai et al. 2012).

The optical selection of QSOs has been performed mainly with follow-up spectroscopic observations of colour–colour-selected candidates (e.g., Croom et al. 2004; Richards et al. 2002a; Pâris et al. 2012; McGreer et al. 2013; Palanque-Delabrouille et al. 2013), using slitless or prism spectroscopic surveys and through inefficient flux-limited spectroscopic surveys (e.g. VIMOS-VLT Deep Survey, Bongiorno et al. 2007). The novel photometric survey definition by COMBO-17 (Wolf et al. 2003) introduced for the first time a highly efficient selection criterion for QSOs with photometric redshift (photo-z) estimates with precisions of $\Delta z/(1+z) \sim 0.03$. Following the same philosophy, the Advanced Large, Homogeneous Area, Medium-Band Redshift Astronomical (ALHAMBRA[1]) survey aims at probing a large cosmological portion of the universe with a deep and wide catalogue of extragalactic sources with highly accurate photometry (Moles et al. 2008). The survey actually covers ~4 deg^{2}over eight different regions of sky and provides a photometric dataset over 20 contiguous, equal-width, non-overlapping, medium-band optical filters (3500–9700 Å) plus the three standard broad-band near-infrared (NIR) filters JHK_S (Benítez et al. 2009; Aparicio Villegas et al. 2010). The capabilities of the ALHAMBRA survey to select and classify extragalactic sources with its *very low-resolution-spectra* have been explored for galaxies and AGN by Molino et al. (2013) and Matute et al. (2012), respectively. The photometric redshift precision achieved is $\Delta z/(1+z) \sim 0.011$ and 0.009 for galaxies and AGNs, respectively. A morphological classification for more than 20 000 ALHAMBRA galaxies (with photo-$z < 1.3$) has been recently derived by Pović et al. (2013).

We present here the discovery of a UV-optically faint QSO at a redshift of 5.41 from the ALHAMBRA photometric survey. The selection criteria and spectroscopic observations are described in Sects. 2 and 3, respectively, while Sect. 4 presents the general properties of the QSO. The significance of our discovery is discussed in Sect. 4 and the conclusions are summarised in Sect. 5. Throughout this paper we assume a ΛCDM cosmology with $H_o = 73\,\mathrm{km\,s^{-1}\,Mpc^{-3}}$, $\Omega_\Lambda = 0.73$, and $\Omega_M = 0.27$. Unless otherwise specified, all magnitudes are given in the AB system.

2. High-z QSOs candidates

Optical i-dropouts have proven useful in detecting high-z QSO (e.g. Fan et al. 2001, based on SDSS photometry). Unfortunately, the i-dropouts and broad-band colours of a $z \sim 5$–6 QSO can look very similar to those of evolved/passive galaxies at $z \sim 1$ or of local red giants and super-giants. Matute et al. (2012) have shown that using the 23 bands of the ALHAMBRA photometric catalogue makes it possible to efficiently classify a high percentage (~90%) of the $z = [0, 3]$ BLAGN/QSO population and measure highly accurate photometric redshifts.

We have applied the methodology described by Matute et al. (2012) to the search for high-z ($z > 5$) QSOs using the ALHAMBRA photometric database. The candidates were selected over ≈1 deg^2 in the two ALHAMBRA fields (out of eight; ALH-2/DEEP2 and ALH-8/SDSS) observable from the Roque de los Muchachos observatory in La Palma during the 2011B semester according to the following criteria: i) located in the fully exposed areas of the images and in regions not contaminated by bright sources flux or artefacts (e.g. spikes); ii) detected (at least) in the three NIR bands and the four reddest optical[2] filters; and iii) having a best-fit template of a BLAGN/QSO (templates numbers 29 to 59 in Matute et al. 2012), and photo-$z \geq 5$ with a probability[3] at the selected redshift >50%. As a result of the spectroscopic follow-up of one of the highest probability candidates, we report the discovery and basic properties of ALH023002+004647, a low-luminosity and very high-redshift QSO. The left-hand panel of Fig. 1 shows the ALH023002+004647 cutouts of the 23 ALHAMBRA filters plus a colour composite.

3. Observations and data reduction

A pilot programme, containing ALH023002+004647, was approved and observed with the OSIRIS[4] spectrograph at the ten-meter GTC telescope located at the Observatorio del Roque de los Muchachos in La Palma. Since only a redshift confirmation and rough spectral classification was required, we used the low-resolution red grism R300R (with a resolution of 327 and a wavelength coverage from 5000 Å to 10 000 Å) with a slit width of 1.2″ and a 2 × 2 on-chip binning. The observations of our candidates were carried out during September and November 2011 (period 2011B) under spectroscopic conditions.

The reduction process made use of standard IRAF/PyRAF facilities. Wavelength calibration was carried out by comparison with exposures of HgAr, Xe, and Ne lamps. We used the 5577 Å [O I] sky emission line to correct (applying a rigid shift) for the small offsets that can be introduced by instrument

[1] http://www.alhambrasurvey.com

[2] Notice that this implies the detection of flux at $8450 < \lambda < 9630$ Å, which induces an upper limit on the redshift $z \lesssim 6$ and a photometric upper limit $m_z \lesssim 22.5$ for this sample.

[3] The photometric redshift code *LePhare* provides the normalised probability distribution over redshift (Pdz) for each source, i.e. at each z (based on the photometry quality, the SED library, and parameters assumptions) Pdz gives the probability that it is the correct one.

[4] http://www.gtc.iac.es/en/pages/instrumentation/osiris.php

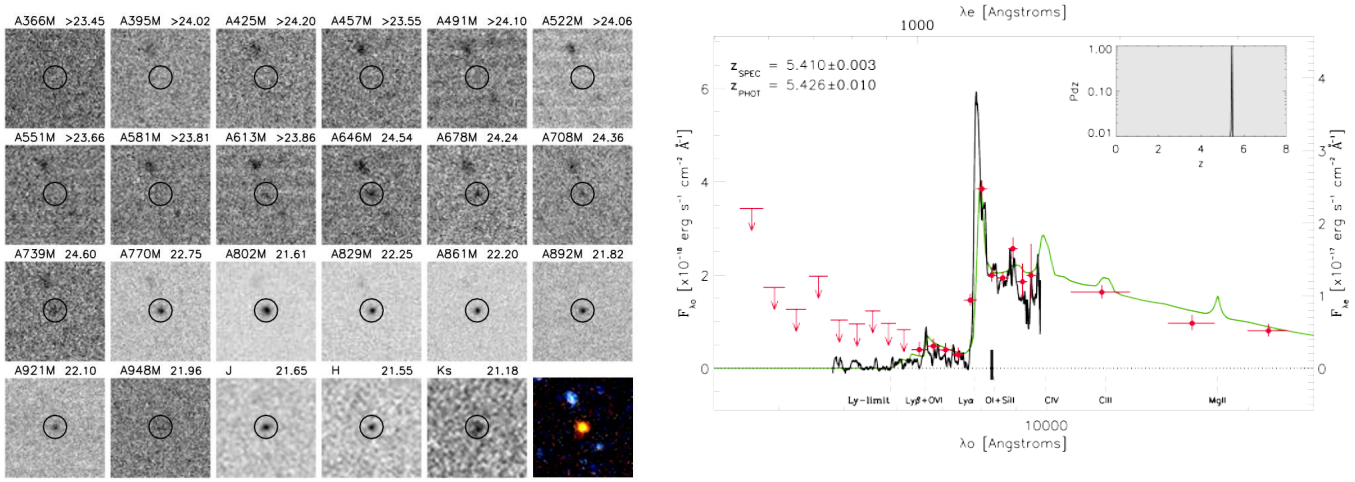

Fig. 1. *Left*: cutouts (15″ × 15″) in all the ALHAMBRA optical/NIR filters for the discovered QSO (highlighted by an open circle). Above each cutout we indicate the filter name and measured magnitude (or 5-σ lower limit). The final image is a colour composite of all bands, where the contrast has been increased to make all objects clearly visible. Images are oriented with north up and east to the left. *Right*: optical-NIR spectral energy distribution of the discovered QSO. ALHAMBRA photometric detections are represented as circles with associated error bars (arrows indicate the 5σ upper limits). The reference magnitude in the m_{830} filter is indicated by a vertical thick line. The best photo-z template solution (QSO with optical slope index $\alpha = -0.25$ at $z_{\rm PHOT} = 5.426 \pm 0.010$) is shown as a green line, while the OSIRIS/GTC spectrum (smoothed with a 7 pixel box) is shown as a thick black line, with the redshift probability function (Pdz) in the inset. The agreement found between the spectro-z and the photo-z is remarkable. The most important emission lines for QSOs at the redshift of the source are also indicated.

flexures. Relative flux calibration was carried out by observations of the spectrophotometric standard stars G158-100 and GRW708247. Each of the four 1200 s exposures was reduced and flux calibrated independently, and they were combined afterward. The final spectrum is the result of 4800 s on-source integration time at a resolution of 6.5 Å/pixel with a continuum signal-to-noise ratio (S/N) of 10 at 1450 Å rest frame. The spectrum after smoothing with a seven pixel-wide boxcar filter is shown in the right-hand panel of Fig. 1, together with the ALHAMBRA photometry and best-fit template model.

4. Properties of ALH023002+004647

The spectrum of ALH023002+004647 shows typical features of a high-z QSO spectrum with a very blue continuum and prominent emission from broad Lyα, N V, Lyβ+O VI and the Si IV+O IV] complex. The continuum bluewards of Lyα is substantially reduced due to intervening clouds of neutral hydrogen present in the inter-galactic medium (IGM) at different redshifts along the line of sight (the Lyα forest). Nevertheless, the presence of a detectable flux blueward of Lyα is a clear sign that the universe was highly ionised at the rest frame of the source.

Table 1 resumes the main characteristics of the identified QSO.

4.1. Redshift

We derived a preliminary spectroscopic redshift $z = 5.410 \pm 0.003$ based on the position of the O I + Si II emission line λ1302. The observed wavelength of Lyβ+O VI is compatible with this redshift.

An alternative approach for measuring the redshift, which allows using the highly asymmetric Lyα + N V complex, consists in modelling the continuum and the strongest emission lines (Lyα, N V and Si II), together with a stochastic realisation of the IGM absorption. The result of such an approach is shown in Fig. 2. The continuum has been normalised as a power law of slope 2.5 (as $F_\lambda \propto \lambda^{-2.5}$). The emission lines have been modelled with single Gaussian profiles at a common redshift $z = 5.42$ for Lyα and N V, and $z = 5.41$ for Si II λ1260. The FWHM of the fitted Lyα is ≈1600 km s^{-1}, well above the ≈1000 km s^{-1} limit offered by the instrumental resolution of the grating we used, and usual for this type of object.

To include the effect of the IGM in the spectrum, we have generated 100 Lyα forest absorption spectra for lines of sight corresponding to the given redshift $z = 5.42$, using the technique

Table 1. Properties of the quasar ALH023002+004647.

ALH-Field	ALH-2 (DEEP2)	(*i*)
RA (J2000)	$02^{\rm hh}\ 30^{\rm mm}\ 02.27^{\rm ss}$	(*ii*)
Dec (J2000)	$+00^{\rm dd}\ 46'\ 46.8''$	(*iii*)
m_{830}	22.25 ± 0.08	(*iv*)
$z_{\rm PHOT}$	5.426 ± 0.014	(*v*)
Best fit SED	qso_0.25 (model #42)	(*vi*)
Best fit $E(B-V)$	0.08	(*vii*)
Best fit Ext. Law	SMC	(*viii*)
$z_{\rm SPEC}$	5.410 ± 0.003	(*ix*)
EW(Lyα)	86	(*x*)
f_{1450}	1.388×10^{-17}	(*xi*)
M_{1450}	-24.07 ± 0.20	(*xii*)
$L_{\rm bol}$	$46.28^{+0.19}_{-0.35}$	(*xiii*)
$M_{\rm BH}$	$(1.52 \pm 0.83) \times 10^8$	(*xiv*)
$\alpha_{\rm O}$	0.25	(*xv*)

Notes. (*i*) ALHAMBRA field name; (*ii*, *iii*) Object coordinates; (*iv*) observed magnitude in the ALHAMBRA A830M filter; (*v*, *vi*, *vii*, *viii*) derived photo-z, template, intrinsic extinction and extinction law from the best fit to the ALHAMBRA photometry (for details see Matute et al. 2012); (*ix*) spectroscopic redshift; (*x*) rest-frame Lyα equivalent width (Å) from our modellisation of the spectrum continuum and emission lines (see Sect. 4.5); (*xi*) rest-frame monochromatic flux at 1450 Å in units of erg s^{-1} cm^{-2} Å^{-1}; (*xii*) absolute magnitude at 1450 Å; (*xiii*) $\log_{10}$ of the bolometric luminosity [erg s^{-1}]; (*xiv*) black hole mass ($M_\odot$) assuming it radiates at the Eddington limit; (*xv*) optical continuum power law index ($f \propto \nu^{-\alpha}$).

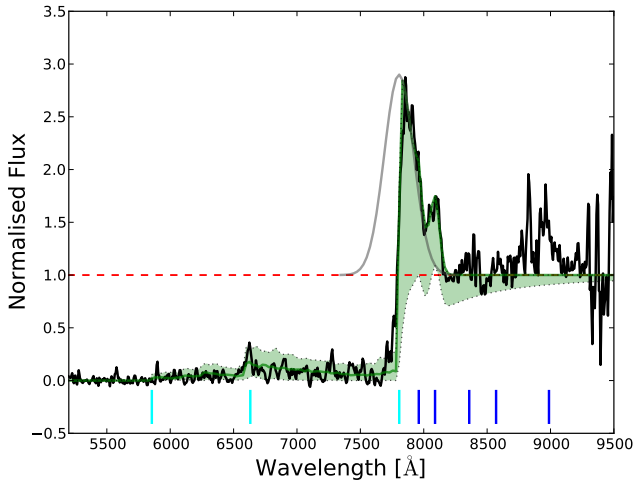

Fig. 2. Modellisation of the observed spectrum divided by the fitted continuum (black line). The Lyα, N V, and Si II λ1260 lines have been modelled with Gaussian profiles. The Gaussian fit to Lyα is shown in grey. The result of dividing the normalised continuum plus the modelled lines by the median absorption, as well as upper and lower 2-σ deviations, generated by simulating 100 IGM sightlines at the same redshift are shown as a continuous (median) and dotted green line (2-σ limits). Vertical cyan lines mark the positions of the Lyman limit, Lyβ, and Lyα lines at the reference redshift. Blue vertical lines mark the expected positions of the N V λ1240, Si II λ1260, O I λ1302, C II λ1335, and (O IV+Si IV)λ1400 emission lines at the same redshift.

presented in Fernández-Soto et al. (2003). These spectra are able to reproduce the average absorption in the Lyα and Lyβ regions, as well as the incidence of Lyman limit and damped Lyα systems and the basic statistical properties of the absorption. For each pixel in the 100 resulting spectra we calculated the resulting median, 1σ and 2σ statistical absorption, and used them to generate the IGM absorption component over our continuum plus emission-line model.

As can be seen in Fig. 2, the model perfectly reproduces the highly asymmetric (Lyα + N V) profile, as well as the average observed flux in the Lyα and Lyβ forest ranges. Only for the 2.5% densest IGM absorption sightlines would the model underestimate the data redward of Lyman α, and this is due to the putative presence, in those cases, of a strong damped Lyα system at a redshift close to that of the quasar itself-a possibility that is clearly discarded by the data.

The Lyα redshift derived with this second method, z = 5.420 ± 0.005, agrees with the O I + Si II estimate within the errors, but we cannot reject the possibility of an offset in the emission-line velocities, as observed in other quasar spectra. We find a small discrepancy between the redshift provided by Lyα and N V, and the low-ionisation emission line. The disagreement is only of the order of ∼500 km s^{-1}, but in a direction opposite to the expected one. We find the low-ionisation lines – supposedly marking the real, systemic redshift – to be blueshifted with respect to our only clearly detected high-ionisation line, N V, which is in a position that is compatible with Lyman α.

As a comparison, Gaskell (1982), in his pioneering work, found an offset of ≈600 km s^{-1} in the opposite direction to the one we find, whereas Richards et al. (2002b) and Shen et al. (2007) used large samples of quasars to find deviations of the same order, albeit with large scatter, covering from −500 out to 2000 km s^{-1} and beyond. Such scatter would, in fact, render the difference observed in ALH023002+004647 compatible with their extreme cases. However, we would need a better spectrum (particularly in terms of S/N) to study the emission lines in more detail.

4.2. Companion galaxies

The cutout images of the QSO (Fig. 1) show two companions located 5″ to the NE and 4″ to the SW. According to the ALHAMBRA catalogue (Molino et al., in prep.), the NE source corresponds to an $AB(I)$ = 23.8 blue galaxy at photometric redshift $z_{\rm ph}$ = 2.25 whose spectrum peaks at ≈6500 Å, and the SW source corresponds to an $AB(I)$ = 25.2 blue galaxy at photometric redshift $z_{\rm ph}$ = 2.10 peaking at ≈5500 Å. The former has a counterpart in the NED database, the source RCS-01020502096 from the Red-Sequence Cluster Survey (Hsieh et al. 2005) with a reported redshift of 0.249. However, the R band magnitude of this object (R = 23.6) puts it well below the limit that Hsieh et al. (2005) quote for good quality redshifts in their catalogue. No other counterpart has been found for the second source. According to our data both sources correspond to low-to-average mass galaxies (log $(M/M_{\odot}) \approx 10.5 \sim 10.8$).

Given the estimated masses for the companions and their distance to the QSO, they should provide negligible gravitational lensing amplification to the QSO image (Willott et al. 2005). We have checked this for the observed configuration (including both redshift possibilities in the case of the NE source), establishing an upper limit to the possible magnification of 0.4%. This may not be exact since the colours of both sources are intrinsically blue, and we used a simple model of an early galaxy type halo – however, no realistic halo model would yield a significantly different result, not over a factor of two in the magnification effect (Bartelmann & Schneider 2001).

4.3. Black hole mass

The best black hole measurements (apart from reverberation mapping) can only be obtained using the FWHM of Hβ or MgII λ2800 as a surrogate (Marziani & Sulentic 2012). Unfortunately, there is no currently available NIR spectra that covers the wavelength range where these lines are located (1.8 and 3.1 μm for MgII and Hβ respectively). Nevertheless, a crude estimation of the black hole mass and bolometric luminosity can be obtained through the rest-frame 1350 Å continuum flux measurement. The observed 1350 Å continuum flux value of $(1.78 \pm 0.27) \times 10^{-18}$ erg s^{-1} cm^{-2} Å^{-1} translates into an absolute luminosity of $(5.03 \pm 0.76) \times 10^{45}$ erg s^{-1} at 1350 Å, assuming an isotropic emission and assuming that the QSO flux has not been magnified by gravitational lensing. A bolometric luminosity of $(1.91 \pm 1.05) \times 10^{46}$ erg s^{-1} was obtained following the prescription given in Richards et al. (2006a) (a 3.8 ± 2.0 factor at log $(\nu) \approx 15.3$ Hz). A black hole mass of $(1.52 \pm 0.83) \times 10^8$ $M_{\odot}$ is derived assuming that the QSO is radiating at the Eddington limit (Peterson 1997). We note that a recent study of high-redshift quasars by Willott et al. (2010a) has shown that assumption to be reasonable, with all nine $z \approx 6$ quasars in their sample having $0.3 < L_{\rm Bol}/L_{\rm Edd} < 2.5$ and $\langle L_{\rm Bol}/L_{\rm Edd} \rangle = 1.3$.

4.4. Ancillary data

There is a detection of ALH023002+004647 by SDSS in the Stripe 82 coadd (SDSS J023002.28+004646.8) with reported magnitudes of 29.00 ± 1.45, 26.62 ± 1.00, 24.31 ± 0.18, 22.64 ± 0.07, and 21.79 ± 010 in the u, g, r, i, and z bands respectively. No optical, ultraviolet, and radio detections by

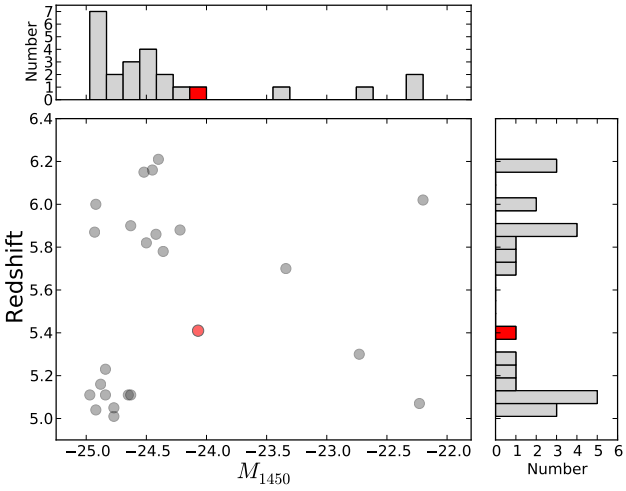

Fig. 3. Luminosity-redshift distribution for the 24 currently known faint ($M_{1450} > -25$) QSOs above $z = 5$. References for the 23 grey-filled circles are: Mahabal et al. (2005, 1 src), Jiang et al. (2009, 4 srcs), Willott et al. (2010b, 6 srcs), Masters et al. (2012, 2 srcs) and McGreer et al. (2013, 10 srcs). ALH023002+004647 is indicated by a red-filled circle and histograms.

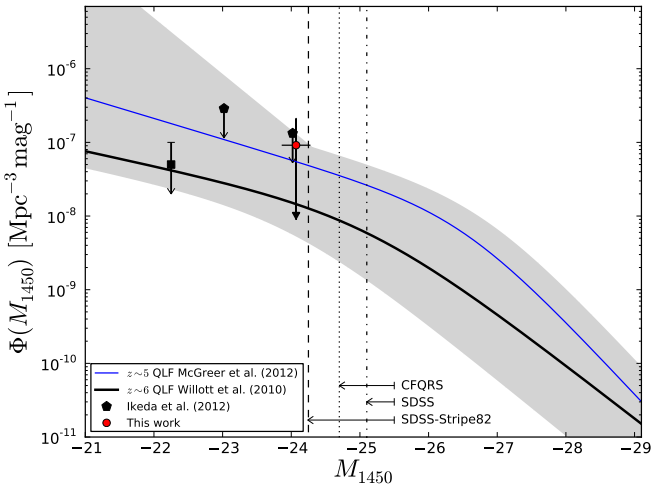

Fig. 4. QSO space density distribution as a function of the rest-frame 1450 Å monochromatic magnitude. The corresponding space density of ALH023002+004647 is represented by the red dot. For comparison with some recent determinations of the high-z QLF, we have plotted the $\langle z \rangle \sim 5$ SDSS-Stripe82 QLF derived by McGreer et al. (2013, blue line) and the $\langle z \rangle \sim 6$ CFQRS+SDSS-Deep QLF derived by Willott et al. (2010b, black line). The vertical lines indicate the faintest magnitude bin sampled by the SDSS-Main, SDSS-Stripe82, and CFQRS. The grey shaded area delimits the range covered by the published QLFs in the redshift bin [5−6] (see text for details). The black pentagons represent the upper limits derived by Ikeda et al. (2012) in the COSMOS field while the black square shows the space density associated to the faintest known QSO above $z = 5$ (Willott et al. 2010b).

HST, GALEX, XMM-OM, and VLA-FIRST are reported by MAST[5] for ALH023002+004647. The Infrared Science Archive (IRSA[6]) provides counterparts above 5-σ from *Spitzer*/IRAC observations at 3.6, 4.5, and 5.8 μm with a 3.8″ aperture flux of 9.56(±0.36), 13.45(±0.57), and 14.17(±2.60) μJy, respectively. These fluxes are compatible, within the errors, with the photo-z best fit solution SED. The sky position of ALH023002+004647 is covered by the Field-4 of the DEEP2 Redshift Survey. Neither the discovered QSO nor the companions have spectroscopic information in the latest data release DR4 (Newman et al. 2012).

The cross-correlation of the ALH023002+004647 position with the high-energy HEASARC[7] and XSA[8] databases reveals that the field has only been observed by *XMM-Newton* with the Epic camera. We find no counterpart associated with the QSO as the closest *XMM-Newton* detection is located 12″ from the QSO and coincides with a galaxy at $z = 0.73$.

5. Discussion

With $M_{1450} = -24.07 \pm 0.2$, ALH023002+004647 is the fifth (out of 24) less luminous QSOs known above redshift of $z = 5$. As a consequence, it samples the faint part ($M_{1450} > -25$) of QLF, which is currently poorly constrained at these redshifts. This is illustrated in Fig. 3 where we have plotted, in the redshift-luminosity space, all the faint spectroscopically confirmed QSO with $z > 5$. Stronger constraints to the space density of high-z low luminosity QSOs are needed to address questions such as the implications for early AGN/host-galaxy interactions or the true fraction of ionizing photons coming from AGN activity in an epoch of increasing QSO activity and significant BH growth. Therefore, in the following we derive the space density associated with the ALH023002+004647 detection.

A first approximation to the contribution of ALH023002+004647 to the $z \approx 5.5$ space density has been computed using the binned $1/V_a$ method of Avni & Bahcall (1980), where V_a is the comoving volume per magnitude and redshift interval accessible to the source, taking the characteristics of the survey into account. It is defined as

$$V_a = \int_{\Delta M} \int_{\Delta z} p(M, z) \frac{dV}{dz} \, dz \, dM,$$

where $p(M, z)$ is the function that corrects for the survey incompleteness at each M and z. The space density associated to ALH023002+004647 is computed as $\Phi(M, z) = 1/V_a$.

The first release of the ALHAMBRA photometric database has been recently finalised and its completeness needs to be addressed through extensive simulations. For the time being, and given our first order approximation, we therefore consider that all "possible" type-I QSOs within the magnitude limits of the survey could have been detected (i.e. $p(M, z) = 1$). We find this to be a reasonable assumption based on previous results for QSO completeness maps of similar surveys like COMBO-17 (see Fig. 4 in Wolf et al. 2003), therefore the volume accessible to our QSO is only delimited by the redshift range $z = [5.0, 6.1]$. At $z \sim 6.1$ the QSO would no longer satisfy our selection criteria, since the magnitude m_{830} would be fainter than ∼25 when it samples the Ly-forest of the spectra. The lower limit redshift is fixed by our requirement to have a best fit model with $z_{PHOT} \geq 5.0$. The necessary K-corrections have been derived using the best-fit template for the photo-z solution.

Considering the covered area (≈1 deg^2) and the magnitude limit of our selection, we derive a space density of $(9.15^{+21.06}_{-9.15}) \times 10^{-8}$ Mpc^{-3} mag^{-1} for ALH023002+004647. The errors were estimated from Poisson statistics (Gehrels 1986). The result is presented in Fig. 4. In order to illustrate the large uncertainties of the high-z QLF, we have delimited the luminosity-density

[5] http://archive.stsci.edu/
[6] http://irsa.ipac.caltech.edu
[7] http://heasarc.gsfc.nasa.gov/
[8] http://xmm.esac.esa.int/xsa/

space covered by several published QLFs in the $z \approx 5-6$ redshift range, namely: CFQRS+SDSS-Deep (Willott et al. 2010b), SDSS-stripe82 (McGreer et al. 2013), COMBO-17 (Wolf et al. 2003) and SDSS-Deep-Stripe (Jiang et al. 2009). Two of the most recent determinations of the QLF at $z = 5$ (McGreer et al. 2013) and $z = 6$ (Willott et al. 2010b) are highlighted. We also report the upper limits derived by Ikeda et al. (2012) from the non-detections of QSOs in the redshift bin [4.5–5.5] of the COSMOS field and the faintest QSO identification above $z = 5$ in the SXDS field as the only constraints to the very faint end of the QLF.

The associated error due to poor statistics hardly constrains the $z \sim 5-6$ QLFs, making our measurement compatible with all the previous, both single and double power law determinations. Nevertheless, the result is very promising considering that the QSO selection was made in a fraction of the total area covered by ALHAMBRA and based on preliminary photometry. With the final release of the ~4 sq. degrees of ALHAMBRA data already in place, our collaboration aims to further constrain the QLF over a much wider range of magnitudes and redshifts.

6. Conclusions

We report the discovery of ALH023002+004647, a new, intrinsically faint, QSO at $z = 5.41$. The candidate was selected based on an SED fitting to the 23 bands of the ALHAMBRA photometry and spectroscopically confirmed with GTC/OSIRIS. The observed continuum luminosity at 1450 Å ($M_{1450} \sim -24$) and derived bolometric luminosity of $\approx 2 \times 10^{46}$ erg s^{-1} make ALH023002+004647 one of the faintest QSOs discovered above $z = 5$. Based on the ALH023002+004647 space density (and associated errors), no tighter constraints can be placed on the $z \sim 5-6$ QLF. Nonetheless, we have demonstrated the capabilities of the ALHAMBRA survey for selecting this type of source. An analysis similar to the one presented here, when applied to the final release of the ALHAMBRA photometric database (DR4) in the near future, will surely make a significant contribution to the QLF at these very high redshifts.

Acknowledgements. Part of this work was supported by Junta de Andalucía, through grant TIC-114 and the Excellence Project P08-TIC-3531, and by the Spanish Ministry for Science and Innovation through grants AYA2006-1456, AYA2010-15169, and AYA2010-22111-C03-02, and Generalitat Valenciana project Prometeo 2008/132. I.M. thanks Cécile Cartozo for the careful reading of the manuscript. This research has made use of the NASA/IPAC Extragalactic Database (NED), which is operated by the Jet Propulsion Laboratory, California Institute of Technology, under contract with the National Aeronautics and Space Administration. Based on observations collected at the Centro Astronómico Hispano Alemán (CAHA) at Calar Alto, operated jointly by the Max-Planck Institut für Astronomie and the Instituto de Astrofísica de Andalucía (CSIC), and on observations with the Gran Telescopio Canarias (GTC), installed in the Spanish Observatorio del Roque de los Muchachos of the Instituto de Astrofísica de Canarias, on the island of La Palma. M.P. acknowledges financial support from the JAE-Doc programme of the Spanish National Research Council (CSIC), co-funded by the European Social Fund.

References

Aparicio Villegas, T., Alfaro, E. J., Cabrera-Caño, J., et al. 2010, AJ, 139, 1242
Avni, Y., & Bahcall, J. N. 1980, ApJ, 235, 694
Bartelmann, M., & Schneider, P. 2001, Phys. Rep., 340, 291
Benítez, N., Moles, M., Aguerri, J. A. L., et al. 2009, ApJ, 692, L5
Bongiorno, A., Zamorani, G., Gavignaud, I., et al. 2007, A&A, 472, 443
Croom, S. M., Smith, R. J., Boyle, B. J., et al. 2004, MNRAS, 349, 1397
Croom, S. M., Richards, G. T., Shanks, T., et al. 2009, MNRAS, 399, 1755
Di Matteo, T., Springel, V., & Hernquist, L. 2005, Nature, 433, 604
Dunkley, J., Komatsu, E., Nolta, M. R., et al. 2009, ApJS, 180, 306
Fan, X., Narayanan, V. K., Lupton, R. H., et al. 2001, AJ, 122, 2833
Fan, X., Strauss, M. A., Becker, R. H., et al. 2006, AJ, 132, 117
Fernández-Soto, A., Lanzetta, K. M., & Chen, H.-W. 2003, MNRAS, 342, 1215
Gaskell, C. M. 1982, ApJ, 263, 79
Gehrels, N. 1986, ApJ, 303, 336
Hopkins, P. F., Croton, D., Bundy, K., et al. 2010, ApJ, 724, 915
Hsieh, B. C., Yee, H. K. C., Lin, H., & Gladders, M. D. 2005, ApJS, 158, 161
Ikeda, H., Nagao, T., Matsuoka, K., et al. 2012, ApJ, 756, 160
Jiang, L., Fan, X., Bian, F., et al. 2009, AJ, 138, 305
Khandai, N., Feng, Y., DeGraf, C., Di Matteo, T., & Croft, R. A. C. 2012, MNRAS, 423, 2397
Mahabal, A., Stern, D., Bogosavljević, M., Djorgovski, S. G., & Thompson, D. 2005, ApJ, 634, L9
Marziani, P., & Sulentic, J. W. 2012, New Astron. Rev., 56, 49
Masters, D., Capak, P., Salvato, M., et al. 2012, ApJ, 755, 169
Matute, I., Márquez, I., Masegosa, J., et al. 2012, A&A, 542, A20
McGreer, I. D., Jiang, L., Fan, X., et al. 2013, ApJ, 768, 105
Melia, F. 2013, ApJ, 764, 72
Moles, M., Benítez, N., Aguerri, J. A. L., et al. 2008, AJ, 136, 1325
Molino, A., Benítez, N., Moles, M., et al. 2013, MNRAS, submitted [arXiv:1306.4968v2]
Newman, J. A., Cooper, M. C., Davis, M., et al. 2012, ApJS, submitted [arXiv:1203.3192]
Palanque-Delabrouille, N., Magneville, C., Yèche, C., et al. 2013, A&A, 551, A29
Pâris, I., Petitjean, P., Aubourg, É., et al. 2012, A&A, 548, A66
Peterson, B. M. 1997, An Introduction to Active Galactic Nuclei (Cambridge Univ. Press)
Pović, M., Huertas-Company, M., Aguerri, A. L., et al. 2013, MNRAS, accepted [arXiv:1308.3146]
Richards, G. T., Fan, X., Newberg, H. J., et al. 2002a, AJ, 123, 2945
Richards, G. T., Vanden Berk, D. E., Reichard, T. A., et al. 2002b, AJ, 124, 1
Richards, G. T., Lacy, M., Storrie-Lombardi, L. J., et al. 2006a, ApJS, 166, 470
Richards, G. T., Strauss, M. A., Fan, X., et al. 2006b, AJ, 131, 2766
Ross, N. P., McGreer, I. D., White, M., et al. 2013, ApJ, 773, 14
Schroeder, J., Mesinger, A., & Haiman, Z. 2013, MNRAS, 428, 3058
Shen, Y., Strauss, M. A., Oguri, M., et al. 2007, AJ, 133, 2222
Siana, B., Polletta, M. D. C., Smith, H. E., et al. 2008, ApJ, 675, 49
Willott, C. J., Percival, W. J., McLure, R. J., et al. 2005, ApJ, 626, 657
Willott, C. J., Albert, L., Arzoumanian, D., et al. 2010a, AJ, 140, 546
Willott, C. J., Delorme, P., Reylé, C., et al. 2010b, AJ, 139, 906
Wolf, C., Wisotzki, L., Borch, A., et al. 2003, A&A, 408, 499